# S0, Where Is It?

Diane M. Papazian

Department of Physiology, David Geffen School of Medicine at UCLA, Los Angeles, CA 90095

The era of high resolution structural analysis of $K^+$ channels began a decade ago when Rod MacKinnon and colleagues reported the x-ray structure of KcsA, a prokaryotic channel comprising four subunits (Doyle et al., 1998). Each subunit of KcsA contains two transmembrane (TM) segments that surround the central pore and an intervening reentrant loop that forms the $K^+$ selectivity filter. The MacKinnon laboratory followed this feat with a series of elegant structures, most recently of a eukaryotic, voltage-dependent $K^+$ (Kv) channel, Kv1.2, and a chimeric channel based on Kv1.2 (Long et al., 2005, 2007). The latter structure is particularly noteworthy because it contains associated lipids that provide a more membrane-like environment for the channel protein (Long et al., 2007).

Before Kv x-ray structures were available, structural constraints identified using indirect biochemical or functional approaches proved useful for generating early structural models (Lainé et al., 2003; Durell et al., 2004). These models suggested experiments to test possible physical mechanisms for channel function. In addition, indirect constraints made predictions about the structural architecture of Kv channels that were later confirmed by x-ray crystallography. This includes the identification of electrostatic interactions between charged residues in the TM segments of the voltage sensor and the prediction that the voltage sensor domain in one Kv subunit interacts with the pore domain of the adjacent subunit in the clockwise direction (Papazian et al., 1995; Tiwari-Woodruff et al., 1997; Lainé et al., 2003). In this regard, the indirect constraints have been essential for evaluating whether structures solved by x-ray crystallography where the channels are embedded in a detergent environment accurately represent functional $K^+$ channels in their native membrane environment. One important example is the original x-ray structure of KvAP, a prokaryotic, voltage-gated $K^+$ channel (Jiang et al., 2003). This structure is hard to reconcile with a diverse array of indirect data (Cohen et al., 2003), and it is now generally accepted that the structure represents a nonnative conformation (Lainé et al., 2003; MacKinnon, 2003). In contrast, there is satisfying agreement between the indirect constraints and more recent Kv structures (Lainé et al., 2003; Long et al., 2005, 2007).

With the availability of Kv x-ray structures, it is now feasible to construct preliminary models of more distantly related $K^+$ channel proteins. Because some of these relatives differ significantly from the Kv family, indirect structural constraints will remain important tools for refining such models. In this issue of the Journal, Liu et al. (see p. 537) report an impressively thorough analysis of the position of S0 in large-conductance, $Ca^{2+}$-activated $K^+$ channels (BK, maxiK, slo) using an engineered disulfide cross-linking strategy. The importance of this work is that S0 is a unique TM segment in BK channels, which affects gating and mediates functional coupling to auxiliary β subunits (Wallner et al., 1996; Meera et al., 1997; Orio et al., 2002).

BK channels are widely expressed and play a significant role in $Ca^{2+}$ signaling (Ghatta et al., 2006; Latorre and Brauchi, 2006; Salkoff et al., 2006). In resting cells, free cytoplasmic $Ca^{2+}$ is low, ~100 nM, due to high concentrations of $Ca^{2+}$ buffering agents, including $Ca^{2+}$ binding proteins. In many cell types, stimulation increases cytoplasmic $Ca^{2+}$ due to entry across the plasma membrane and/or release from intracellular stores. BK channels serve as negative feedback regulators of $Ca^{2+}$ entry, particularly through voltage-dependent pathways including voltage-gated $Ca^{2+}$ channels and ryanodine receptors (Latorre and Brauchi, 2006; Salkoff et al., 2006). BK channels open in response to increases in cytoplasmic $Ca^{2+}$, causing an efflux of $K^+$ that hyperpolarizes the cell, shutting off depolarization-evoked $Ca^{2+}$ influx.

BK channels are notable for single channel conductances exceeding 200 pS in symmetrical 100 mM $K^+$ and for their dual regulation by voltage and intracellular $Ca^{2+}$ (Latorre and Brauchi, 2006; Salkoff et al., 2006). These channels open in response to membrane depolarization and/or increases in cytoplasmic $Ca^{2+}$. Voltage and $Ca^{2+}$ act largely independently to increase the probability of opening (Po) and either can act alone to gate BK channels. Under physiological conditions, however, depolarization and increased $Ca^{2+}$ must coincide to achieve a high Po. In resting cells with typical hyperpolarized membrane potentials and low free $Ca^{2+}$, the Po of endogenous BK channels is exceedingly small; Po values of 50% are attained only at unphysiological voltages

Correspondence to Diane M. Papazian: papazian@mednet.ucla.edu

Abbreviation used in this paper: TM, transmembrane.


The Rockefeller University Press $30.00
J. Gen. Physiol. Vol. 131 No. 6 531–536
www.jgp.org/cgi/doi/10.1085/jgp.200810031

(>+100 mV) (Latorre and Brauchi, 2006; Salkoff et al., 2006). In contrast, in the presence of 1–5 μM $Ca^{2+}$, the Po of endogenous BK channels approaches 100% at voltages attained during a typical action potential (Latorre and Brauchi, 2006; Salkoff et al., 2006). Low micromolar concentrations of free $Ca^{2+}$ may be achieved only in the immediate vicinity of $Ca^{2+}$ entry sites because the high buffering capacity of the cytoplasm limits $Ca^{2+}$ diffusion. Not surprisingly, therefore, BK channels are often localized in proximity to $Ca^{2+}$ channels, including voltage-gated $Ca^{2+}$ channels at neuronal synapses and ryanodine receptors in smooth endoplasmic reticulum (Orio et al., 2002). Thus, BK channels are situated to take advantage of microdomains of high $Ca^{2+}$ immediately adjacent to major sites of $Ca^{2+}$ entry.

The molecular constituents of BK channels have been identified (Salkoff et al., 2006). Four α subunits, which are structurally related to Kv subunits, assemble to form the central, $K^+$-selective permeation pathway. Each α subunit contains a voltage sensor domain. In most cells, α subunits associate in a 1:1 stoichiometry with auxiliary β subunits, which modulate the functional properties and pharmacology of BK channels (Orio et al., 2002).

The first gene for a BK α subunit was cloned from *Drosophila* using a genetic approach (Atkinson et al., 1991). The α subunit gene is mutated in *slowpoke* flies, resulting in locomotor abnormalities and temperature-sensitive lethargy (Elkins et al., 1986; Atkinson et al., 1991). In mammals, there is one α subunit gene (Slo1, KNCMA1) that is subject to extensive alternative splicing, increasing the functional diversity of BK channels (Salkoff et al., 2006). The genome also encodes three related proteins (Slo2–Slo4) that do not form voltage- and $Ca^{2+}$-gated channels (Salkoff et al., 2006).

BK α subunits contain the major structural hallmarks of Kv proteins, including six TM segments (S1–S6) and a reentrant loop that forms the $K^+$ selectivity filter (Meera et al., 1997; Latorre and Brauchi, 2006; Salkoff et al., 2006). TM segments S1–S4 contribute to the voltage sensor domain, and the pattern of charged residues in S2, S3, and S4 is well conserved (Fig. 1). S4 contains several positively charged arginine residues that in Kv channels are responsible for sensing changes in voltage (Aggarwal and MacKinnon, 1996; Seoh et al., 1996). However, BK α subunits diverge from Kv channel proteins in two important ways. First, the BK α subunit has a large C-terminal domain that constitutes approximately two thirds of the protein (Atkinson et al., 1991). $Ca^{2+}$ sensitivity is conferred by high affinity binding sites in the C terminus (Salkoff et al., 2006). Second, the topology of the membrane domain differs from that of Kv channels due to the presence of an additional TM segment, S0, preceding S1 (Wallner et al., 1996; Meera et al., 1997). As a result, the N terminus of the BK α subunit is extracellular, in contrast to the cytoplasmic location found in Kv channels.

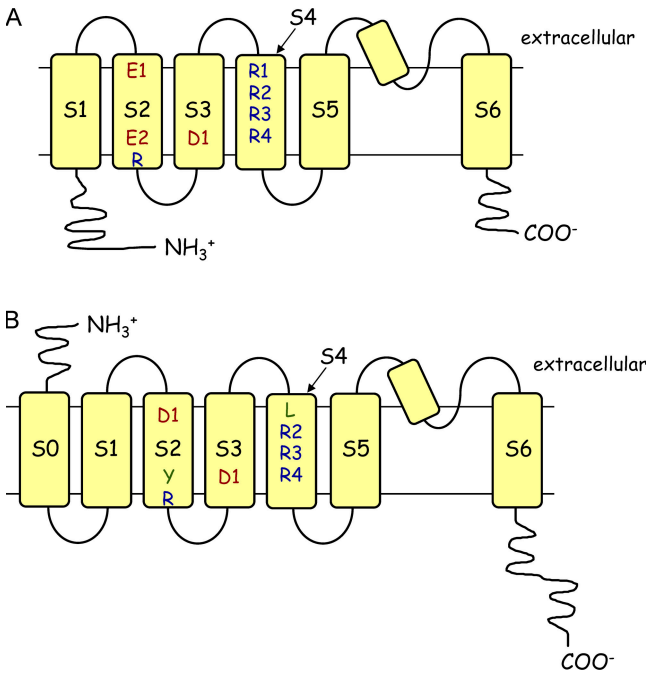


**Figure 1.** Topology and charged residues in the voltage sensor domain in Kv (A) and BK (B) subunits. (A) Kv subunits comprise six TM segments (S1–S6), a reentrant selectivity filter loop, and intracellular N and C termini. (B) BK α subunits comprise seven TM segments (S0–S6), a reentrant selectivity filter loop, an extracellular N terminus, and an intracellular C terminus. Positively and negatively charged residues are shown in blue and red, respectively. Neutral residues are shown in green. The pattern of charged residues in S2, S3, and S4 is conserved between Kv and BK α subunits with the following exceptions: in BK channels, E1 in S2 is replaced by D1; E2 in S2 is replaced by Y; R1 in S4 is replaced by L. A sequence alignment of the murine BK α subunit and a representative Kv subunit, Kv1.2, is shown in Fig. 1 of Liu et al., 2008.

BK α subunits associate with auxiliary β subunits in a tissue-specific manner (Orio et al., 2002). The first β subunit was identified because it copurified with the BK α subunit (Knaus et al., 1994). Subsequent molecular analysis revealed that four genes encode the β1–β4 subunits (Orio et al., 2002). BK β subunits are glycosylated membrane proteins with intracellular N and C termini and two TM segments. β subunits modify the functional properties of BK channels. β1 shifts the Po-V curve in the hyperpolarized direction and decreases its slope. These changes in the voltage dependence of gating result in an apparent increase in $Ca^{2+}$ sensitivity. Coassembly with β1 subunits also slows the kinetics of activation and deactivation, and alters the sensitivity of the channel to charybdotoxin. Coexpression of α with β2 or β3 confers fast, N-type inactivation on BK channels.

The unique extracellular N terminus and S0 TM segment of the BK α subunit are required for functional coupling to β (Wallner et al., 1996). To understand the

mechanism by which β subunits modulate BK gating and kinetics, it is important to determine the location of S0 relative to the rest of the channel. The report by Marx and colleagues (Liu et al., 2008) provides a major advance in our knowledge about the structural relationship between S0 and the other TM segments in the BK α subunit. The strategy was to identify disulfide bonds formed between pairs of engineered cysteine residues, with one cysteine located near the extracellular end of S0 and the other located near the extracellular end of one of the other TM segments in the α subunit. Because the rate of disulfide formation increases with proximity and can be affected by protein flexibility and the local electrostatic potential (Careaga and Falke, 1992), efficient disulfide formation was interpreted as structural proximity between the cysteine residues. Extrapolating from the structure of Kv channels, in which the voltage sensor from one subunit is close to the pore domain in an adjacent subunit (Long et al., 2005, 2007), the authors anticipated that both intra- and intersubunit disulfide bonds might be detected.

Intersubunit disulfide bonds between $K^+$ channel subunits are easily detected on SDS-PAGE because monomers and oligomers have significantly different mobilities (Lainé et al., 2003). In contrast, intrasubunit disulfide bonds are challenging to detect. Although intrasubunit disulfides sometimes alter the mobility or appearance of the monomer band, no such changes were observed for the BK α subunit. Instead, the authors used a clever and effective strategy to identify intrasubunit bonds (Liu et al., 2008). A cleavage site for the HRV-3C protease was inserted in the intracellular S0–S1 loop so that proteolysis would separate S0 from the rest of the TM segments in the α subunit. In the presence of reducing agents, the proteolytic fragments migrate as bands of 110 and 15 kD. In the absence of a disulfide bond, the same bands would be seen under nonreducing conditions. However, in the presence of an intrasubunit disulfide bond between the two fragments, the cleaved protein would migrate as a monomer of 125 kD under nonreducing conditions.

The analysis of disulfide bond formation by Liu et al. is an experimental tour de force. Individual cysteine mutations were made at positions flanking S0–S6 on the extracellular side of the membrane in the murine BK α subunit. Mutations included four each in the sequences extracellular to S0, S1, and S2; each position of the short, four-residue linker between S3 and S4; eight residues extracellular to S5, and six residues extracellular to S6. Double cysteine constructs included one pre-S0 mutation plus one other mutation elsewhere in the α subunit. In all, 47 pairs of cysteine mutations were investigated. To avoid detecting spurious disulfide bonds in intracellularly retained, misfolded protein, the analysis was restricted to protein expressed at the plasma membrane. Cell surface proteins were biotinylated with a relatively impermeant reagent and isolated on Neutravidin beads before HRV-3C protease treatment and SDS-PAGE under reducing and nonreducing conditions. The 125-kD BK α subunit and its 110-kD proteolytic fragment were detected on immunoblots using an antibody directed against the C terminus.

Intrasubunit disulfide bonds were detected between S0 and residues elsewhere in the voltage sensor domain (Liu et al., 2008). The highest extent of disulfide bond formation (estimated to be ≥90%) was found between any of the four pre-S0 cysteine mutations and two positions in the S3–S4 loop. The fact that four sequential residues showed equivalent levels of cross-linking with the same two positions in the S3–S4 loop suggests that the region immediately preceding S0 is not in a fixed α-helical or β-strand secondary structure. Significant reaction between residues flanking S0 and S1, and S0 and S2 was also observed. These results are compatible with the identification of an endogenous disulfide bond between C14 in the N terminus and C141 in the S1–S2 loop. (These endogenous cysteines were mutated to alanine in the engineered cysteine constructs.)

In contrast, disulfide bonds did not form efficiently between cysteines near S0 and in the pore domain (Liu et al., 2008). Since S0 and voltage sensor residues form intrasubunit disulfide bonds, intersubunit disulfide bonds would be expected between S0 and pore residues (Lainé et al., 2003; Long et al., 2005). These experiments were complicated by the fact that mutant subunits containing two cysteine residues, one of which was in the pore domain, were retained inside the cell, suggesting aberrant folding or assembly. Therefore, the experiments were conducted by coexpressing single mutant subunits. One subunit had a cysteine near S0, whereas the other subunit had a cysteine in the pore domain. This strategy reduces the extent of disulfide bonding that could be obtained since only some subunit arrangements would be expected to cross-link. However the authors detected virtually no formation of intersubunit disulfide bonds and concluded that S0 is not located near the pore domain. This is logical given the substantial body of data that places S0 in proximity to S1–S4.

Since the functional coupling of α and β subunits requires the N terminus and S0 (Wallner et al., 1996), the authors compared disulfide bond formation in the presence and absence of β subunits (Liu et al., 2008). No significant differences were found, and β retained its ability to modulate gating in channels containing intrasubunit disulfide bonds in the α subunit.

The results indicate that S0 associates with the rest of the voltage sensor domain in the BK α subunit. Adapting a model of the closed state of Kv1.2 (Yarov-Yarovoy et al., 2006), Liu et al. present a model in which S0 is integrated into the voltage sensor domain, close to S3 and S4 since this is where disulfide bond formation was most

efficient. To account for significant cross-linking with the S1–S2 loop, S0 is inserted between S2 and S3. This model is compatible with the large dataset acquired with engineered disulfide bonds and with the endogenous disulfide bond between the N terminus and the S1–S2 loop.

Liu et al. (2008) report the functional effects of disulfide bond formation in some of the constructs with the highest extent of cross-linking. Some had functional properties similar to those of the wild-type channel, whereas others affected the voltage dependence and kinetics of gating. The striking finding, however, is that all of the disulfide-bonded channels were able to open and close. This result suggests that the S0 TM segment remains closely associated with the rest of the voltage sensor domain during voltage-dependent gating. The data are consistent with the idea that the amplitude of voltage sensor conformational changes is relatively small, but other explanations cannot be excluded. In Kv channels, the nature and amplitude of voltage sensor conformational changes remain a matter of debate (Tombola et al., 2006).

Positioned between S2 and S3, as suggested by Liu et al. (2008), S0 would be in an excellent location to modulate voltage sensor function based on what we know about voltage-dependent gating in Kv channels. The exquisite voltage sensitivity of Kv channels is conferred primarily by the first four arginine residues in the S4 TM segment (R1–R4 in Fig. 1 A) (Aggarwal and MacKinnon, 1996; Seoh et al., 1996). These residues must traverse a significant fraction of the transmembrane electric field to account for the 12–13 elementary charges that are transferred by voltage sensor conformational changes during the activation of a single channel (Schoppa et al., 1992). In addition to R1–R4, a conserved glutamate near the intracellular end of S2 (E2 in Fig. 1 A) has been implicated in the voltage-sensing process, although its role is not well understood (Seoh et al., 1996). Although the nature of voltage sensor conformational changes is not yet clear, there is emerging recognition that another conserved glutamate in S2 (E1 in Fig. 1 A) interacts electrostatically with the charge-moving S4 arginine residues in different conformational states. From biochemical and functional evidence, it was proposed some time ago that E1 in S2 interacts with R3 in an intermediate closed state and with R4 in the activated conformation (Tiwari-Woodruff et al., 2000; Silverman et al., 2003). The electrostatic interaction between E1 and R4 in the activated state was recently confirmed by the x-ray structure of Kv1.2 (Long et al., 2005). Additional evidence suggests that E1 interacts with R1 when the voltage sensor is in its resting conformation (Tombola et al., 2007). Taken together the results suggest that E1 serves as an electrostatic way station for charge-moving S4 residues during voltage-dependent activation.

Mathematically, Kv gating is well described by kinetic models containing at least two voltage-dependent conformational changes per subunit (Zagotta et al., 1994). Once the four voltage sensors are in the activated conformation, the cytoplasmic pore gate opens in a forward-biased, cooperative transition.

How similar are the mechanisms of voltage-dependent gating in Kv and BK channels? The pattern of charged residues in S2, S3, and S4 is generally well conserved, although the BK α subunit lacks R1 in S4, and E2 in S2 has been replaced by tyrosine (Fig. 1 B). In BK channels, four charged residues have been implicated in voltage sensing but only one, corresponding to R4, is located in the S4 segment (Fig. 1 B) (Ma et al., 2006; see also Díaz et al., 1998). The others are D1 and R in S2 and D1 in S3 (Fig. 1 B).

$Ca^{2+}$-dependent gating of BK channels, in contrast, is mediated by the large C-terminal cytoplasmic domain of the α subunit (Latorre and Brauchi, 2006; Salkoff et al., 2006). $Ca^{2+}$ sensing is conferred by two high affinity binding sites, one in the $Ca^{2+}$ bowl, which contains a sequence of negatively charged amino acids, and the other in the RCK (regulator of conductance of $K^+$) domain. The RCK domain is thought to form a gating ring that controls the position of the cytoplasmic pore gate in S6 (Jiang et al., 2002). The pore gate and the RCK domain are mechanically coupled by the linker between them, which functions as an elastic spring (Niu et al., 2004). $Ca^{2+}$ binding and voltage sensor activation are thought to increase the tension in the spring, pulling on the gate and increasing the probability of channel opening. The conformational changes of the linker and the gating ring during activation are unknown, however.

The functional properties of BK gating are well described by a kinetic model containing three allosterically coupled transitions, corresponding to voltage sensor conformational changes between resting and activated states, $Ca^{2+}$ binding, and pore opening (Horrigan and Aldrich, 2002). This model has been useful for understanding mechanistically the functional changes seen in mutant channels.

A previous report suggests that S0 affects voltage sensor movement in BK channels, consistent with the location of S0 proposed by Liu et al. (2008). Tryptophan scanning mutagenesis of the S0 TM segment indicates that F25W, L26W, and S29W cause large positive shifts in the voltage dependence of gating (Koval et al., 2007). These shifts are observed in the presence or absence of $Ca^{2+}$, suggesting that they result from changes in the equilibrium constant between resting and activated conformations of the voltage sensor. Assuming that S0 is an α helix starting at M21, F25 would be slightly more than one helical turn from the preS0 residues (R17, G18, Q19, R20) targeted for cysteine mutagenesis by Liu et al. (2008). The high impact residues F25, L26, and

S29 are invariant from flies to mammals and cluster with other highly conserved residues on one face of the S0 α helix (Koval et al., 2007). This side of S0 may interact with other TM segments in the voltage sensor domain. Alternatively, this face may interact with the β subunit, since S0, along with the N terminus, is required for functional coupling to β (Wallner et al., 1996). Physical association between the α and β subunits appears to require the α N terminus as well as TM segments in the voltage sensor domain (Morrow et al., 2006). The orientation of the S0 TM segment and more detailed mapping of the location of β relative to the α subunit are interesting questions for future studies.

Considering possible differences between voltage-dependent gating in BK and Kv channels, it is intriguing that the model of Marx and colleagues places S0 between S2 and S3. In Kv channels, this region of the voltage sensor domain is a hot spot for gating modulation. In ether-à-go-go and HERG channels, divalent cations bind between S2 and S3 to modulate activation and deactivation gating, respectively (Silverman et al., 2000; Lin and Papazian, 2007). Gating modifier toxins, which alter voltage sensor conformational changes, interact with the extracellular end of S3 (Li-Smerin and Swartz, 2001). Gating modifier toxins have been identified not only for Kv channels but also for voltage-dependent $Na^+$ and $Ca^{2+}$ channels (Catterall et al., 2007; McDonough, 2007; Swartz, 2007).

Gating modulators in Kv channels regulate voltage sensor conformational changes but do not appear to change the basic mechanism of activation or the identity of the voltage sensing residues (Silverman et al., 2003). In contrast, the identities of voltage sensing residues in BK and Kv channels differ significantly (Aggarwal and MacKinnon, 1996; Ma et al., 2006; Seoh et al., 1996). Could this be due, at least in part, to the insertion of S0 in the BK voltage sensor domain? An interesting but highly speculative possibility is that the presence of S0 changes the spatial relationship between S2 and S4, affecting state-dependent electrostatic interactions between E1 in S2 and voltage-sensing arginines in S4. This might alter the structure of the voltage sensor in resting and activated conformations and shift some of the task of sensing voltage to charged residues outside S4.

In summary, the work of Marx and colleagues increases our understanding of the structural organization of BK channels and provides some insight into how the unique N terminus and S0 TM segment might affect voltage-dependent gating and its modulation by β subunits.

## REFERENCES


Aggarwal, S.K., and R. MacKinnon. 1996. Contribution of the S4 segment to gating charge in the Shaker $K^+$ channel. *Neuron.* 16:1169–1177.

Atkinson, N.S., G.A. Robertson, and B. Ganetzky. 1991. A component of calcium-activated potassium channels encoded by the *Drosophila slo* locus. *Science.* 253:551–555.

Careaga, C.L., and J.J. Falke. 1992. Thermal motions of surface α-helices in the D-galactose chemosensory receptor. Detection by disulfide trapping. *J. Mol. Biol.* 226:1219–1235.

Catterall, W.A., S. Cestèle, V. Yarov-Yarovoy, F.H. Yu, K. Konoki, and T. Scheuer. 2007. Voltage-gated ion channels and gating modifier toxins. *Toxicon.* 49:124–141.

Cohen, B.E., M. Grabe, and L.Y. Jan. 2003. Answers and questions from the KvAP structures. *Neuron.* 39:395–400.

Díaz, L., P. Meera, J. Amigo, E. Stefani, O. Álvarez, L. Toro, and R. Latorre. 1998. Role of the S4 segment in a voltage-dependent calcium-sensitive potassium (hSlo) channel. *J. Biol. Chem.* 273:32430–32436.

Doyle, D.A., J. Morais Cabral, R.A. Pfuetzner, A. Kuo, J.M. Gulbis, S.L. Cohen, B.T. Chait, and R. MacKinnon. 1998. The structure of the potassium channel: molecular basis of $K^+$ conduction and selectivity. *Science.* 280:69–77.

Durell, S.R., I.H. Shrivastava, and H.R. Guy. 2004. Models of the structure and voltage-gating mechanism of the Shaker $K^+$ channel. *Biophys. J.* 87:2116–2130.

Elkins, T., B. Ganetzky, and C.-F. Wu. 1986. A *Drosophila* mutation that eliminates a calcium-dependent potassium current. *Proc. Natl. Acad. Sci. USA.* 83:8415–8419.

Ghatta, S., D. Nimmagadda, X. Xu, and S.T. O'Rourke. 2006. Large-conductance, calcium-activated potassium channels: structural and functional implications. *Pharmacol. Ther.* 110:103–116.

Horrigan, F.T., and R.W. Aldrich. 2002. Coupling between voltage-sensor activation, $Ca^{2+}$ binding and channel opening in large conductance (BK) potassium channels. *J. Gen. Physiol.* 120:267–305.

Jiang, Y., A. Lee, J. Chen, M. Cadene, B.T. Chait, and R. MacKinnon. 2002. Crystal structure and mechanism of a calcium-gated potassium channel. *Nature.* 417:515–522.

Jiang, Y., A. Lee, J. Chen, V. Ruta, M. Cadene, B.T. Chait, and R. MacKinnon. 2003. X-ray structure of a voltage-dependent $K^+$ channel. *Nature.* 423:33–41.

Knaus, H.G., M. Garcia-Calvo, G.J. Kaczorowski, and M.L. Garcia. 1994. Subunit composition of the high conductance calcium-activated potassium channel from smooth muscle, a representative of the mSlo and slowpoke family of potassium channels. *J. Biol. Chem.* 269:3921–3924.

Koval, O.M., Y. Fan, and B.S. Rothberg. 2007. A role for the S0 transmembrane segment in voltage-dependent gating of BK channels. *J. Gen. Physiol.* 129:209–220.

Lainé, M., M.A. Lin, J.P.A. Bannister, W.R. Silverman, A.F. Mock, B. Roux, and D.M. Papazian. 2003. Atomic proximity between S4 segment and pore domain in Shaker potassium channels. *Neuron.* 39:467–481.

Latorre, R., and S. Brauchi. 2006. Large conductance $Ca^{2+}$-activated $K^+$ (BK) channel: activation by $Ca^{2+}$ and voltage. *Biol. Res.* 39:385–401.

Lin, M.A., and D.M. Papazian. 2007. Differences between ion binding to eag and HERG voltage sensors contribute to differential regulation of activation and deactivation gating. *Channels.* 1:429–437.

Li-Smerin, Y., and K.J. Swartz. 2001. Helical structure of the COOH terminus of S3 and its contribution to the gating modifier toxin receptor in voltage-gated ion channels. *J. Gen. Physiol.* 117:205–218.

Liu, G., S.I. Zakharov, L. Yang, S.-X. Deng, D.W. Landry, A. Karlin, and S.O. Marx. 2008. Position and role of the BK channel α subunit S0 helix inferred from disulfide crosslinking. *J. Gen. Physiol.* 131:537–548.

Long, S.B., E.B. Campbell, and R. MacKinnon. 2005. Crystal structure of a mammalian voltage-dependent Shaker family $K^+$ channel. *Science.* 309:897–903.

Long, S.B., X. Tao, E.B. Campbell, and R. MacKinnon. 2007. Atomic structure of a voltage-dependent $K^+$ channel in a lipid membrane-like environment. *Nature.* 450:376–382.

Ma, Z., X.J. Lou, and F.T. Horrigan. 2006. Role of charged residues in the S1-S4 voltage sensor of BK channels. *J. Gen. Physiol.* 127:309–328.

MacKinnon, R. 2003. Potassium channels. *FEBS Lett.* 555:62–65.

McDonough, S.I. 2007. Gating modifier toxins of voltage-gated calcium channels. *Toxicon.* 49:202–212.

Meera, P., M. Wallner, M. Song, and L. Toro. 1997. Large conductance voltage- and calcium-dependent $K^+$ channel, a distinct member of voltage-dependent ion channels with seven N-terminal transmembrane segments (S0-S6), an extracellular N terminus, and an intracellular (S9-S10) C terminus. *Proc. Natl. Acad. Sci. USA.* 94:14066–14071.

Morrow, J.P., S.I. Zakharov, G. Liu, A.J. Sok, and S.O. Marx. 2006. Defining the BK channel domains required for β1-subunit modulation. *Proc. Natl. Acad. Sci. USA.* 103:5096–5101.

Niu, X., X. Qian, and K.L. Magleby. 2004. Linker-gating ring complex as passive spring and $Ca^{2+}$-dependent machine for a voltage- and $Ca^{2+}$-activated potassium channel. *Neuron.* 42:745–756.

Orio, P., P. Rojas, G. Ferreira, and R. Latorre. 2002. New disguises for an old channel: MaxiK channel β subunits. *News Physiol. Sci.* 17:156–161.

Papazian, D.M., X.M. Shao, S.-A. Seoh, A.F. Mock, Y. Huang, and D.H. Wainstock. 1995. Electrostatic interactions of S4 voltage sensor in Shaker $K^+$ channel. *Neuron.* 14:1293–1301.

Salkoff, L., A. Butler, G. Ferreira, C. Santi, and A. Wei. 2006. High-conductance potassium channels of the SLO family. *Nat. Rev. Neurosci.* 7:921–931.

Schoppa, N.E., K. McCormack, M.A. Tanouye, and F.J. Sigworth. 1992. The size of gating charge in wild-type and mutant Shaker potassium channels. *Science.* 255:1712–1715.

Seoh, S.A., D. Sigg, D.M. Papazian, and F. Bezanilla. 1996. Voltage-sensing residues in the S2 and S4 segments of the Shaker $K^+$ channel. *Neuron.* 16:1159–1167.

Silverman, W.R., B. Roux, and D.M. Papazian. 2003. Structural basis of two-stage voltage-dependent activation in $K^+$ channels. *Proc. Natl. Acad. Sci. USA.* 100:2935–2940.

Silverman, W.R., C.-Y. Tang, A.F. Mock, K.-B. Huh, and D.M. Papazian. 2000. $Mg^{2+}$ modulates voltage-dependent activation in ether-à-go-go potassium channels by binding between transmembrane segments S2 and S3. *J. Gen. Physiol.* 116:663–677.

Swartz, K.J. 2007. Tarantula toxins interacting with voltage sensors in potassium channels. *Toxicon.* 49:213–230.

Tiwari-Woodruff, S.K., C.T. Schulteis, A.F. Mock, and D.M. Papazian. 1997. Electrostatic interactions between transmembrane segments mediate folding of Shaker potassium channel subunits. *Biophys. J.* 72:1489–1500.

Tiwari-Woodruff, S.K., M.A. Lin, C.T. Schulteis, and D.M. Papazian. 2000. Voltage-dependent structural interactions in the Shaker $K^+$ channel. *J. Gen. Physiol.* 115:123–138.

Tombola, F., M.M. Pathak, and E.Y. Isacoff. 2006. How does voltage open an ion channel? *Annu. Rev. Cell Dev. Biol.* 22:23–52.

Tombola, F., M.M. Pathak, P. Gorostiza, and E.Y. Isacoff. 2007. The twisted ion-permeation pathway of a resting voltage-sensing domain. *Nature.* 445:546–549.

Wallner, M., P. Meera, and L. Toro. 1996. Determinant for β-subunit regulation in high-conductance voltage-activated and $Ca^{2+}$-sensitive $K^+$ channels: an additional transmembrane region at the N terminus. *Proc. Natl. Acad. Sci. USA.* 93:14922–14927.

Yarov-Yarovoy, V., D. Baker, and W.A. Catterall. 2006. Voltage sensor conformations in the open and closed states in ROSETTA structural models of $K^+$ channels. *Proc. Natl. Acad. Sci. USA.* 103:7292–7297.

Zagotta, W.N., T. Hoshi, and R.W. Aldrich. 1994. Shaker potassium channel gating. III: Evaluation of kinetics models for activation. *J. Gen. Physiol.* 103:321–362.